

Linear theory of MHD Taylor-Couette flow

Günther Rüdiger

Astrophysikalisches Institut Potsdam, An der Sternwarte 16, D-14482 Potsdam, Germany

Abstract. The linear theory of MHD Taylor-Couette flow (subject to an axial magnetic field and unbounded in z) is presented in order to prepare laboratory experiments to probe the MRI. Only stationary flow patterns are considered but also with nonaxisymmetry and for small magnetic Prandtl numbers. If the outer cylinder is at rest for a small interval of magnetic field amplitudes subcritical excitation is found but only for $\text{Pm} > 1$. For rotating outer cylinder beyond the Rayleigh line the situation is different. Characteristic minima are found for the Reynolds number of the inner cylinder for Hartmann numbers of order 10 for $\text{Pm} = 1$ and 1000 for $\text{Pm} = 10^{-5}$. The minimal *magnetic* Reynolds number in all these cases is of order 10 (see Fig. 7). For liquid sodium ($\text{Pm} = 10^{-5}$) the characteristic values for a container with $R_{\text{in}} = R_{\text{out}}/2 = 10$ cm are 20 Hz for the inner rotation frequency and 1700 Gauss for the magnetic field amplitude.

INTRODUCTION

Consider the Taylor-Couette flow between concentric rotating cylinders for viscous fluids. The rotation law in the container is

$$\Omega(R) = a + \frac{b}{R^2}, \quad (1)$$

where a and b are related to the angular velocities Ω_{in} and Ω_{out} of the inner and the outer cylinders. With R_{in} and R_{out} as the radii of the cylinders one finds

$$a = \frac{\hat{\mu} - \hat{\eta}^2}{1 - \hat{\eta}^2} \Omega_{\text{in}}, \quad b = \frac{1 - \hat{\mu}}{1 - \hat{\eta}^2} \Omega_{\text{in}} R_{\text{in}}^2 \quad (2)$$

with $\hat{\mu} = \Omega_{\text{out}}/\Omega_{\text{in}}$ and $\hat{\eta} = R_{\text{in}}/R_{\text{out}}$. According to the Rayleigh criterion the ideal flow is stable when the specific angular momentum increases outwards, i.e.

$$\hat{\mu} > \hat{\eta}^2. \quad (3)$$

The viscosity, however, stabilizes the flow so that for $\hat{\mu} < \hat{\eta}^2$ it becomes unstable only if the inner cylinder rotates sufficiently fast.

If the fluid is electrically conducting and an axial magnetic field is applied then the critical value grows with growing magnetic field. Figure 1 shows the theoretical results of Chandrasekhar (1961) together with the experimental data for Mercury of Donnelly & Ozima (1960) for narrow gaps and very small magnetic Prandtl numbers. Theory and observations are in nearly perfect agreement with no indication of any magnetic-induced instability. The magnetic Prandtl number under laboratory conditions is really very small.

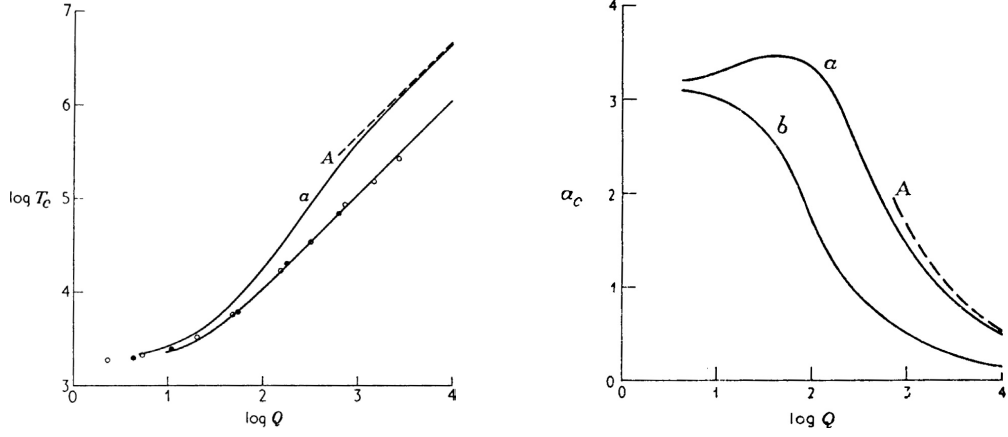


FIGURE 1. Early results for small gap and small Pm (Chandrasekhar 1961). Left: The influence of the magnetic field (Q here the Hartmann number) on the critical Taylor number. Magnetic fields suppress the instability. Right: The same for the wave number. The magnetic field elongates the Taylor vortices in the vertical direction. Boundary conditions: (a) conducting walls, (b) insulating walls.

Within the small-gap approximation but with free Pm Kurzweg (1963) found that for *weak* magnetic fields and sufficiently large magnetic Prandtl number the critical Taylor number becomes *smaller* than in the hydrodynamic case (Fig. 2). If the field is not too strong it can basically play a destabilizing role. For the ideal magnetic Taylor-Couette flow this was first discovered by Velikhov (1959).

In the MHD regime the Rayleigh criterion for stability, Eq. (3), changes to

$$\hat{\mu} > 1, \quad (4)$$

i.e. only flows with superrotation are stable in the MHD regime (Velikhov, his Fig. 1). Velikhov found a growth rate along the Rayleigh line (i.e. $a = 0$) of $2\Omega_{\text{in}}\hat{\eta}$ and a critical ('dangerous') wave number of $k \leq 2\Omega_{\text{in}}\hat{\eta}/V_A$, with V_A the Alfvén velocity of the given axial field. A dispersion relation has been derived for the Fourier frequency ω which can be negative (indicating instability) only if V_A is *smaller* than the shear $-R^2 d\Omega/dR$. The instability, therefore, is a weak-field instability. Chandrasekhar (1960) confirmed these results.

The hydrodynamic Taylor-Couette flow is stable if its angular momentum increases with radius, but the hydromagnetic Taylor-Couette flow is only stable if the angular velocity itself increases with radius. This remains true also for nonideal fluids. The MRI reduces the critical Reynolds number for weak magnetic field strengths for hydrodynamically unstable flow and it destabilizes the otherwise hydrodynamically stable flow for $\hat{\eta}^2 < \hat{\mu} < 1$. The MRI exists, however, in hydrodynamically unstable situations ($\hat{\mu} < \hat{\eta}^2$) only if Pm is not very small (Fig. 2).

As we shall demonstrate, the critical Reynolds numbers vary as $1/\text{Pm}$ for hydrodynamically stable flows so that finally the magnetic Reynolds number Rm controls the instability (see Fig. 7). Because of the high value of η for liquid metals (exceeding $1000 \text{ cm}^2/\text{s}$), it is not easy to reach magnetic Reynolds numbers of the required order of 10. This is the basic reason why the MRI has not yet been observed experimentally in the laboratory.

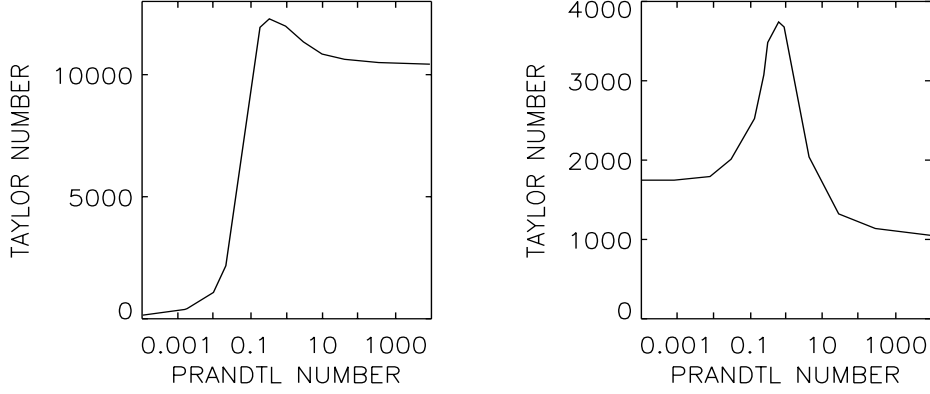


FIGURE 2. Critical Taylor number as a function of the magnetic Prandtl number for strong (left) and weak (right) magnetic fields (small-gap approximation). For weak fields and large magnetic Prandtl numbers the system is subcritical. For $B_0 = 0$ (or, what is the same, for $Pm = 0$) is $Ta_{\text{crit}} = 1750$. (Kurzweg (1963).

THE EQUATIONS

A viscous electrically-conducting incompressible fluid between two rotating infinite cylinders in the presence of a uniform axial magnetic field admits the basic solution $U_R = U_z = B_R = B_\phi = 0$ and

$$B_z = B_0 = \text{const}, \quad U_\phi = aR + \frac{b}{R}, \quad (5)$$

where \mathbf{U} is the velocity, \mathbf{B} is the magnetic field and a and b are given by (2). R , ϕ , and z are the cylindrical coordinates. We are interested in the stability of this solution. The perturbed state of the flow is described by

$$u'_R, R\Omega + u'_\phi, u'_z, B'_R, B'_\phi, B_0 + B'_z. \quad (6)$$

The linear stability problem is considered in full generality with nonaxisymmetric perturbations. By developing the disturbances into normal modes, the solutions of the linearized MHD equations are considered in the form

$$\mathbf{u}' = \mathbf{u}(R)e^{i(m\phi+kz+\omega t)}, \quad \mathbf{B}' = \mathbf{B}(R)e^{i(m\phi+kz+\omega t)}. \quad (7)$$

The equations have been derived by Chandrasekhar (1960) and Roberts (1964). Only different normalizations are used here.

The general form of the induction equation is

$$\frac{\partial \mathbf{B}}{\partial t} = \text{rot}(\mathbf{u} \times \mathbf{B}) + \eta \Delta \mathbf{B} \quad (8)$$

with η as the magnetic diffusivity considered as uniform. One has also to use the additional relation $\text{div } \mathbf{B} = 0$ and $\text{div } \mathbf{u} = 0$. The momentum equation is

$$\rho \left(\frac{\partial \mathbf{u}}{\partial t} + (\mathbf{u} \nabla) \mathbf{u} \right) = -\nabla P + \rho \nu \Delta \mathbf{u} + \mathbf{J} \times \mathbf{B}. \quad (9)$$

Let $D = R_{\text{out}} - R_{\text{in}}$ be the gap between the cylinders. $H = (R_{\text{in}} D)^{1/2}$ is used as the unit of length, the velocity η/H as the unit of the velocity fluctuation, ν/H^2 as the unit of frequencies, B_0 as the unit of the magnetic field fluctuations, H^{-1} as the unit of the wave number and Ω_{in} as the unit of the Ω . The dimensionless numbers of the problem then are the magnetic Prandtl number

$$\text{Pm} = \frac{\nu}{\eta}, \quad (10)$$

the Hartmann number Ha and the Reynolds number Re of the inner rotation, i.e.

$$\text{Ha} = \frac{B_0 H}{\sqrt{\mu_0 \rho \nu \eta}}, \quad \text{Re} = \frac{\Omega_{\text{in}} H^2}{\nu}. \quad (11)$$

Only marginal stability and stationary modes are here considered, i.e. $\omega = 0$. Using the same symbols for normalized quantities, the equations can be written as a system of 10 equations of first order, i.e.

$$\frac{du_R}{dR} = -\frac{u_R}{R} - i\frac{m}{R}u_\phi - ik u_z, \quad \frac{du_\phi}{dR} = X_2 - \frac{u_\phi}{R}, \quad (12)$$

$$\frac{du_z}{dR} = X_3, \quad (13)$$

$$\begin{aligned} \frac{dX_1}{dR} = & \left(\frac{m^2}{R^2} + k^2 \right) u_R + i(\omega + m\text{Re}\Omega)u_R + \\ & + 2i\frac{m}{R^2}u_\phi - 2\text{Re}\Omega u_\phi - ik\text{Ha}^2 B_R, \end{aligned} \quad (14)$$

$$\begin{aligned} \frac{dX_2}{dR} = & \left(\frac{m^2}{R^2} + k^2 \right) u_\phi + i(\omega + m\text{Re}\Omega)u_\phi - \\ & - 2i\frac{m}{R^2}u_R + 2a\text{Re}u_R - ik\text{Ha}^2 B_\phi + \\ & + \frac{m^2}{R^2}u_\phi + k\frac{m}{R}u_z - i\frac{m}{R}X_1, \end{aligned} \quad (15)$$

$$\begin{aligned} \frac{dX_3}{dR} = & \left(\frac{m^2}{R^2} + k^2 \right) u_z + i(\omega + m\text{Re}\Omega)u_z - \\ & - \frac{X_3}{R} - ik\text{Ha}^2 B_z + k\frac{m}{R}u_\phi + k^2 u_z - ikX_1, \end{aligned} \quad (16)$$

$$\frac{dB_R}{dR} = -\frac{B_R}{R} - i\frac{m}{R}B_\phi - ikB_z, \quad \frac{dB_\phi}{dR} = X_4 - \frac{B_\phi}{R}, \quad (17)$$

$$\frac{dB_z}{dR} = i \left(\frac{m^2}{kR^2} + k \right) B_R - \frac{\text{Pm}}{k} (\omega + m\text{Re}\Omega) B_R + u_R - \frac{m}{kR} X_4, \quad (18)$$

$$\begin{aligned} \frac{dX_4}{dR} = & \left(\frac{m^2}{R^2} + k^2 \right) B_\phi + i\text{Pm}(\omega + m\text{Re}\Omega)B_\phi - \\ & - 2i\frac{m}{R^2}B_R - ik u_\phi + 2\text{PmRe}\frac{b}{R^2}B_R. \end{aligned} \quad (19)$$

X_1 is given by

$$X_1 = \frac{du_R}{dR} + \frac{u_R}{R} - P - \text{Ha}^2 B_z \quad (20)$$

with P as the pressure fluctuation.

A set of 10 boundary conditions is needed. Always no-slip conditions for the velocity on the walls are used, i.e. $u_R = u_\phi = du_R/dR = 0$. The boundary conditions depend on the electrical properties of the walls. The tangential currents and the radial component of the magnetic field vanish on conducting walls hence $dB_\phi/dR + B_\phi/R = B_R = 0$.

For insulating walls the magnetic boundary conditions are different at R_{in} and R_{out} , i.e. for R_{in}

$$B_R + i\frac{B_z}{I_m(kR)} \left(\frac{m}{kR} I_m(kR) + I_{m+1}(kR) \right) = 0, \quad (21)$$

and for $R = R_{\text{out}}$

$$B_R + i\frac{B_z}{K_m(kR)} \left(\frac{m}{kR} K_m(kR) - K_{m+1}(kR) \right) = 0, \quad (22)$$

where I_m and K_m are the modified Bessel functions. The condition for the toroidal field is $k_R B_\phi = m B_z$ (Rüdiger, Schultz & Shalybkov 2003).

The homogeneous set of equations with the boundary conditions determine the eigenvalue problem of the form $\mathcal{L}(k, m, \text{Re}, \text{Ha}, \Re(\omega)) = 0$ for given Pm . \mathcal{L} is a complex quantity, both its real part and its imaginary part must vanish for the critical Reynolds number (Fig. 3). The real part, $\Re(\omega)$, of ω describes a drift of the pattern along the azimuth. It is the second quantity fixed by the complex eigenequation. For a fixed Hartmann number, a fixed Prandtl number and a given vertical wave number we find the eigenvalue Re of the system. They are always minimal for a certain wave number defining the marginally unstable mode. The corresponding value of Re is the critical Reynolds number.

RESULTS

Subcritical Excitation for Large Pm

Figure 4 shows the neutral stability for axisymmetric modes for containers with both conducting and insulating walls with resting outer cylinder and for fluids of various magnetic Prandtl number. $\text{Re} = 68$ is the classical hydrodynamic solution. There is a strong difference of the bifurcation lines for $\text{Pm} \gtrsim 1$ (high conductivity) and $\text{Pm} < 1$ (low conductivity). For fluids with low electrical conductivity the magnetic field only suppresses the instability so that all the critical Reynolds numbers exceed the value 68.

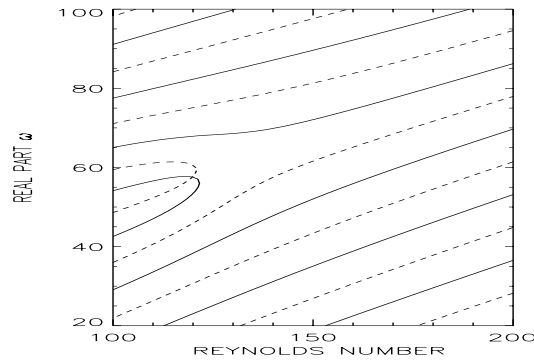


FIGURE 3. Zeros of the real and the imaginary parts of the matrix of the complex eigenequation. At the crossing both parts simultaneously vanish providing the critical Reynolds number and the azimuthal pattern drift.

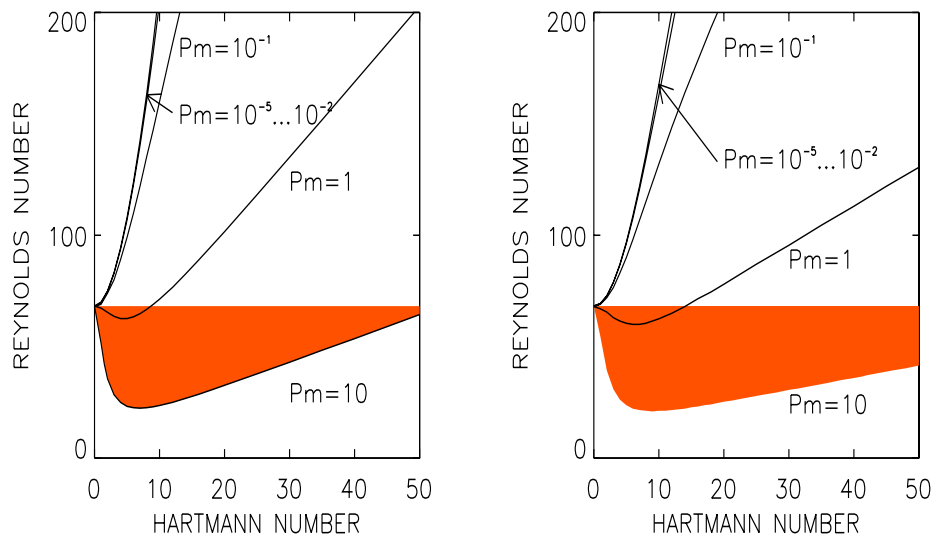


FIGURE 4. Bifurcation diagram for axisymmetric modes with resting outer cylinder of conducting material (left) and vacuum (right). Shaded areas denote subcritical excitation by the axial magnetic field (Rüdiger, Schultz & Shalybkov 2003).

For small magnetic Prandtl number the stability lines hardly differ. The opposite is true for $Pm \gtrsim 1$. In Fig. 4 the resulting critical Reynolds numbers are smaller than $Re = 68$. The magnetic field with small Hartmann numbers enhance the instability rather than suppress it. This effect becomes more effective for increasing Pm but it vanishes for stronger magnetic fields. The MRI only exists for weak magnetic fields and high enough electrical conductivity and/or microscopic viscosity.

The Rayleigh line $a = 0$

There is a particular scaling for the special case for $\hat{\mu} = \hat{\eta}^2$, i.e. with $a = 0$ in the basic flow profile of Eq. (1). Then the term with a vanishes in the equation (14) and for $m = \omega = 0$ one finds that the quantities u_R, u_z, B_R and B_z scale as $\text{Pm}^{-1/2}$ while u_ϕ, B_ϕ, k and Ha scale as Pm^0 . Then the Reynolds number for the axisymmetric modes scales as

$$\text{Re} \propto \text{Pm}^{-1/2}. \quad (23)$$

This scaling does not depend on the boundary conditions. This result has been found numerically for vacuum boundary conditions by Willis & Barenghi (2002). However, for $a > 0$ the much steeper scaling $\text{Re} \propto \text{Pm}^{-1}$ results (see Fig. 7), leading to the surprisingly simple relation

$$\text{Rm} = \frac{\Omega_{\text{in}} R_{\text{in}} D}{\eta} \propto \text{const.} \quad (24)$$

for the magnetic Reynolds number Rm . For the Hartmann number of the characteristic minima we find $\text{Ha} \propto \text{Pm}^{-1/2}$ so that

$$\text{S} \propto \text{const.} \quad (25)$$

results for the Lundquist number $\text{S} = \text{Ha} \sqrt{\text{Pm}}$. For small magnetic Prandtl numbers the exact value of the microscopic viscosity is thus *not* relevant for the instability. In consequence, the corresponding Reynolds numbers for the MRI seem to differ by 2 orders of magnitude, i.e. 10^4 and 10^6 . Experiments with $\hat{\mu} = \hat{\eta}^2$ thus seem to look much more promising than experiments with $\hat{\mu} > \hat{\eta}^2$.

However, this possibility cannot be utilized. The critical Reynolds number for $\hat{\mu} = \hat{\eta}^2$ and $\text{Pm} = 1$ as a function of $\hat{\eta}$ has the absolute minimum $\text{Re} = 54.4$ for $\hat{\eta} = 0.27$, so that according to (23) one expects the value $1.7 \cdot 10^4$ for the Reynolds number for $\text{Pm} = 10^{-5}$. Figure 5 shows the behavior close to $\hat{\mu} = \hat{\eta}^2$. There is a vertical jump from 10^4 to 10^6 within an extremely small interval of $\hat{\mu}$. This sharp transition does not exist for $\text{Pm} = 1$; it only exists for very small values of Pm .

From the jump profile for $\text{Pm} = 10^{-5}$ in Fig. 5 (right) follows that experiments with $\hat{\mu} = \hat{\eta}^2$ are not possible. Even the smallest deviation from the condition $\hat{\mu} = \hat{\eta}^2$ would drastically change the excitation condition.

Rotating outer cylinder

Now the outer cylinder may rotate so fast that the rotation law no longer fulfills the Rayleigh criterion and a solution for $\text{Ha} = 0$ does not exist. The nonmagnetic eigenvalue along the vertical axis moves to infinity but *a minimum remains*. Figure 6 presents the results for $\text{Pm} = 1$ and $\text{Pm} = 10^{-5}$. There are always minima of Re for certain Hartmann numbers (Rüdiger & Shalybkov 2002, Goodman & Ji 2002). The minima and the critical Hartmann numbers increase for decreasing magnetic Prandtl numbers. For $\hat{\eta} = 0.5$ and

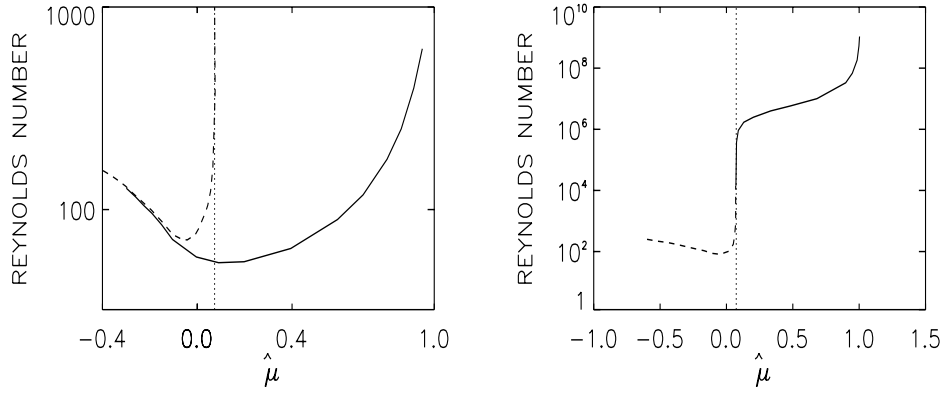


FIGURE 5. Critical Reynolds numbers for the Taylor-Couette flow vs. $\hat{\mu}$ for $\hat{\eta} = 0.27$ and $Pm = 1$ (left) and $Pm = 10^{-5}$ (right). From all $\hat{\eta}$, $\hat{\eta} = 0.27$ yields the lowest minimum. The curve for the hydrodynamic instability ($Ha = 0$) is dashed and the hydromagnetic curve ($Ha > 0$) is solid. The dotted lines denote the location of $a = 0$.

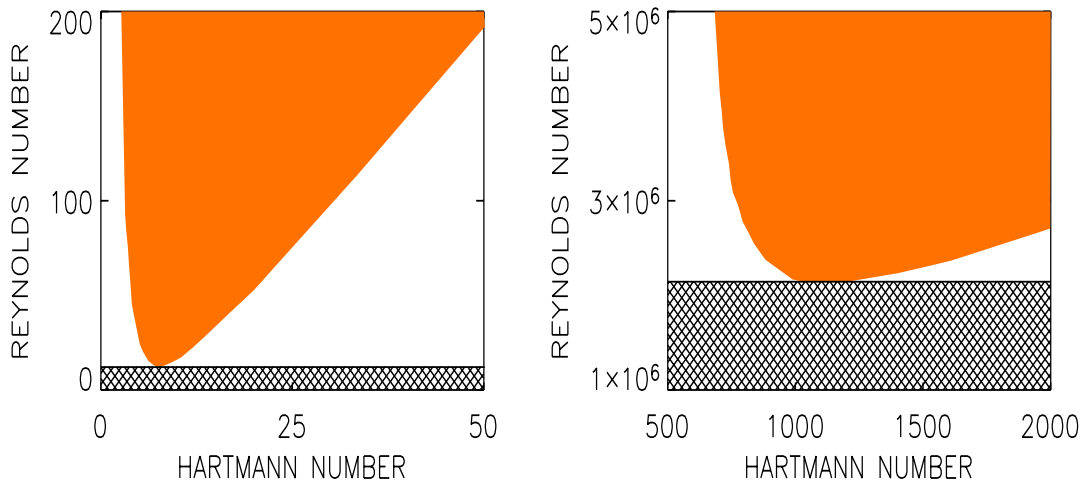


FIGURE 6. Marginal stability lines for axisymmetric modes in containers with rotating outer cylinder of conducting material for $Pm = 1$ (left) and $Pm = 10^{-5}$ (right). $\hat{\eta} = 0.5$, $\hat{\mu} = 0.33$. The instability domain is colored by grey and fluids in the cross-hatched area are always stable.

$\hat{\mu} = 0.33$ the critical Reynolds numbers together with the critical Hartmann numbers are plotted in Fig. 7. Table 1 gives the exact coordinates of the absolute minima for experiments with rotating outer cylinder and for $Pm = 10^{-5}$. They are characterized by magnetic Reynolds numbers of order 10, very similar to the values of the existing dynamo experiments.

TABLE 1. Coordinates of the absolute minima in Fig. 6 for rotating outer cylinder with $\hat{\mu} = 0.33$, $\hat{\eta} = 0.5$ and $\text{Pm} = 10^{-5}$.

	insulating walls	conducting walls
Reynolds number	$1.42 \cdot 10^6$	$2.13 \cdot 10^6$
mag. Reynolds number	14	21
Hartmann number	1400	1100
Lundquist number	4.42	3.47

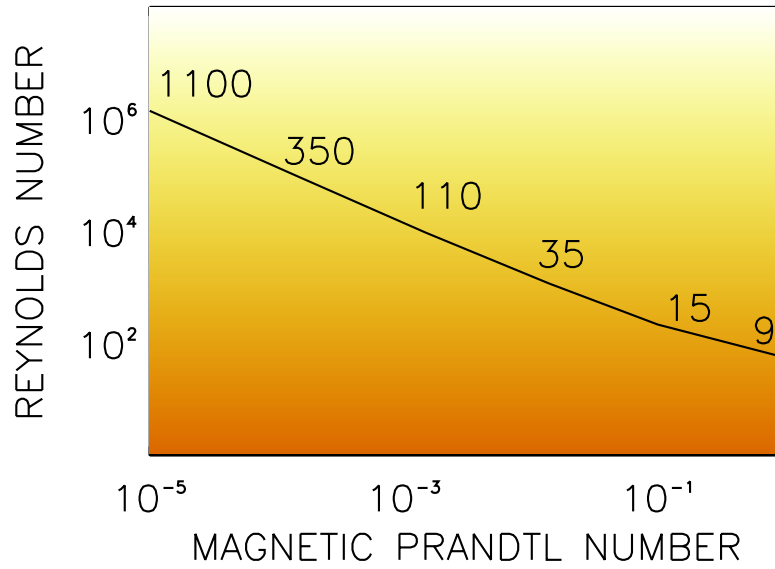


FIGURE 7. The critical Reynolds numbers vs. magnetic Prandtl numbers marked with those Hartmann numbers where the Reynolds number is minimum. $\hat{\eta} = 0.5$, $\hat{\mu} = 0.33$. Rüdiger & Shalybkov (2002).

For liquid sodium in a container with insulating walls we find the critical numbers

$$f_{\text{in}} = 64 \frac{\text{Re}/10^6}{(R_{\text{out}}/10\text{cm})^2} \text{ Hz}, \quad B_0 = \frac{2.2 \text{ Ha}}{R_{\text{out}}/10\text{cm}} \text{ Gauss}, \quad (26)$$

with f_{in} as the real frequency of the inner cylinder and B_0 as the necessary external field. A container with an outer radius of 22 cm (and an inner radius of 11 cm) filled with liquid sodium, therefore, requires a *rotation of about 19 Hz* in order to find the MRI. Following Eq. (26) and the values of Table 1 the required magnetic field is about 1400 Gauss.

The results for containers with *conducting* walls are also given in Table 1. The minimal Reynolds numbers are higher than for insulating cylinder walls. The influence of the boundary conditions is thus not small.

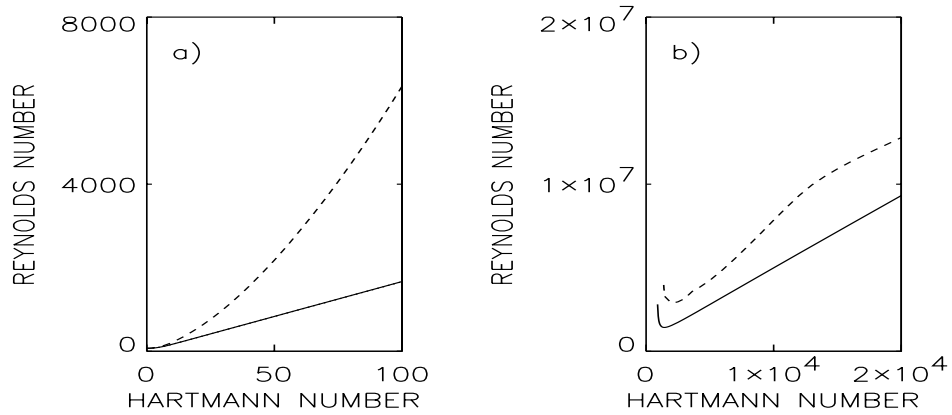


FIGURE 8. Insulating walls (vacuum): Stability lines for $m = 0$, solid lines) and for $m = 1$ (dashed). Left: $\hat{\mu} = 0$. Right: $\hat{\mu} = 0.33$. $\text{Pm} = 10^{-5}$, $\hat{\eta} = 0.5$.

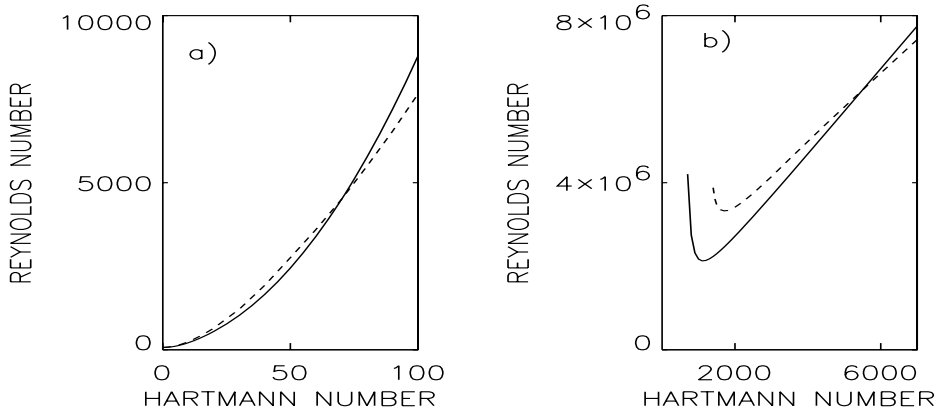


FIGURE 9. The same as in Fig. 8 but for conducting walls. The $m = 1$ mode is preferred for stronger magnetic fields. Shalybkov, Rüdiger & Schultz (2002).

Nonaxisymmetric modes

With respect to future dynamo experiments it is important to know the excitation conditions of nonaxisymmetric modes. After the Cowling theorem only nonaxisymmetric magnetic fields can be maintained by a dynamo process. We start with the results for containers with insulating walls and outer cylinders at rest and for $\text{Pm} = 10^{-5}$ (Fig. 8, left). There are linear instabilities even without magnetic fields. For $\text{Ha} = 0$ solutions for $m = 0$ ($\text{Re} = 68$), $m = 1$ ($\text{Re} = 75$) and $m = 2$ ($\text{Re} = 127$) are known. The axisymmetric mode possesses the lowest Reynolds number. This is also true in the MHD regime: we do not find any crossover of the bifurcation lines for axisymmetric and nonaxisymmetric modes. The same is true for containers with rotating outer cylinder (Fig. 8, right).

There is a basic difference between the two sorts of boundary conditions. For conduction walls we find crossovers of the instability lines for $m = 0$ and $m = 1$ (Fig. 9). For both resting and rotating outer cylinders critical Hartmann numbers exist above which the nonaxisymmetric mode possesses a lower Reynolds number than the axisymmetric mode. The occurrence of nonaxisymmetric solutions as the preferred modes is a rather general phenomenon for containers with conducting walls.

Vertical cell structure

The vertical extension δz of a Taylor vortex is given by

$$\frac{\delta z}{R_{\text{out}} - R_{\text{in}}} = \frac{\pi}{k} \sqrt{\frac{\hat{\eta}}{1 - \hat{\eta}}}. \quad (27)$$

The dimensionless vertical wave numbers k associated with the critical Reynolds numbers are given in Fig. 10. For hydrodynamically unstable flows we have $\delta z \simeq R_{\text{out}} - R_{\text{in}}$ for small magnetic fields ($\text{Ha} \simeq 0$). The cell therefore has the same vertical extent as it has in radius.

The influence of strong magnetic fields on turbulence consists of suppression and deformation. The deformation consists in an elongation of the cell in the vertical direction, so that δz is expected to become larger and larger (the wave number becomes smaller and smaller) for increasing magnetic field. This is indeed true for $\text{Pm} \simeq 1$, but for smaller Pm the vertical cell size has a minimum for an intermediate value of the magnetic field.

The cell size is minimum for the critical Reynolds number for all calculated examples of hydrodynamically stable flows with a conducting boundary. This is not true, however, for containers with insulating walls, for which the cell size grows with increasing magnetic field. For experiments with the critical Reynolds numbers the vertical cell size is generally 2–3 times larger than the radial one. The smaller the magnetic Prandtl number the longer are the cells in the vertical direction.

The influence of boundary conditions on the cell size disappears, of course, for sufficiently wide gaps. For the small and medium gaps, however, one finds the cells vertically more elongated for containers with insulating walls (Fig. 10).

REFERENCES

1. Chandrasekhar, S., *Proc. Nat. Acad. Sci.*, **46**, 53 (1960).
2. Chandrasekhar, S., *Hydrodynamic and Hydromagnetic Stability*, Oxford University Press (1961).
3. Donnelly, R.J., Ozima, M., *Phys. Rev. Lett.*, **4**, 497 (1960).
4. Goodman, J., Ji, H., *JFM*, **462**, 365 (2002).
5. Kurzweg, U.H., *JFM*, **17**, 52 (1963).
6. Roberts, P.H., *Proc. Camb. Phil. Soc.*, **60**, 635 (1964).
7. Rüdiger, G., Shalybkov, D., *Phys. Rev. E*, **66**, 016307 (2002).
8. Rüdiger, G., Schultz, M., Shalybkov, D., *Phys. Rev. E*, **67**, 046312 (2003).
9. Shalybkov, D., Rüdiger, G., Schultz, M., *A&A*, **395**, 339 (2002).
10. Velikhov, E.P., *Sov. Phys. JETP*, **9**, 995 (1959).
11. Willis, A.P., Barenghi, C.F., *A&A*, **393**, 339 (2002).

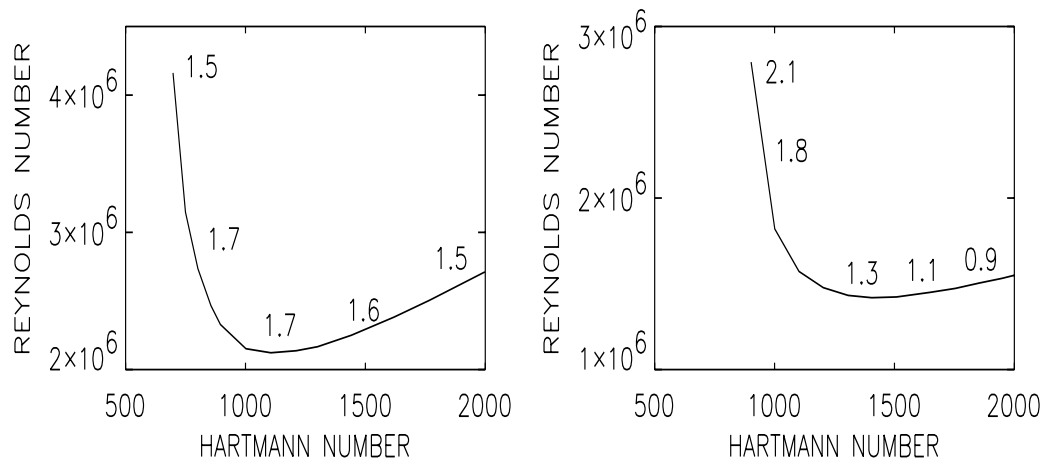


FIGURE 10. The stability line for $\hat{\eta} = 0.5$, $\hat{\mu} = 0.33$ and $Pm = 10^{-5}$. There is no hydrodynamic instability. The line is marked with those wave numbers for which the Reynolds number is minimum. Left: Conducting walls. Right: Insulating walls. Note the differences for different boundary conditions.